ABSTRACT

Rear Projection Screens; A Theoretical Analysis

[redacted] STAT

The increasing use of rear projection screens has necessitated the need for a better understanding of their performance limits based on an analytical model which relates the physical and optical properties of the screen. A general discussion of the optical and viewing properties of rear projection screens, using an operational terminology, is given, and a theoretical model, based on the Mie theory of light scattering, is postulated. Basic light scattering data are used to calculate relations between such optical properties as screen brightness, axial gain, uniformity, efficiency, color fidelity, and ambient light sensitivity from such physical parameters as scattering particle size, number density, and refractive index of the scattering particles relative to the embedding material.

Data from experimental investigations of volume scattering materials, fabricated by Corning Glass Works, are found to be in good agreement with the theoretical calculations.

I. Introduction

The growing use of rear projection screens in all types of displays has generated a need for a sound theoretical understanding of the relationships between the physical parameters of the screen material and the associated optical viewing properties. The compromises imposed by different viewing requirements are known and have been discussed in a number of papers;[1-12] however, the relations between the physical and the optical properties and the limits of performance are notably absent.

A general discussion of the optical and viewing properties is given and a theoretical model for calculating the important properties of such screens is postulated. This analysis is restricted to volume scattering materials, i.e., those which rely on the scattering of light within a volume of material rather than at a single surface or

by a single element. The results of an experimental program to test the validity of the theoretical model and to identify potentially good rear projection screen materials are discussed. A brief comparison is made between these Corning screen materials and some of the available commercial rear projection screens.

II. Background

The function of a rear projection screen is to accept an image from a projector located on one side and to display this image to viewers on the opposite side. The screen must interact with the image, hence the physical properties of the screen material are responsible for the screen's viewing characteristics. In addition to the projection screen, the overall effectiveness of rear projection displays is governed by other factors such as 1) the type of projection, e.g. from slides or motion pictures, from CRT projectors or from laser beam scanners, etc., 2) projection and viewing geometries, e.g. the size of the screen and the size and shape of the viewing area, 3) screen brightness, 4) the level of ambient illumination, and 5) the observer.[13-19] For example, the screen used with a microscope projector is viewed by a single observer positioned directly in

front of the screen, and thus a highly directional screen is required. In general, this type of screen will be efficient and not sensitive to ambient light. On the other hand, a compact unit with a short focal length projection lens and a widely spread audience requires a wide angle screen which backscatters more light, making the screen less efficient and more sensitive to ambient light.

The behavior of a typical rear projection screen is illustrated in Fig. 1. Two rays of light are shown incident on a screen, one in the center at point A, the other at the edge at point B. Continuation of the line representing the incident ray through any point at the screen establishes the 'principle axis' for that particular ray. The angular intensity distribution for any point at the screen has its axis collinear with the corresponding principle axis. An observer located at O will view point A along its principle axis, but will

view point B at some off axis angle θ_B. The angle θ_B is termed the 'bend angle' and along with the angular intensity distribution determines the brightness and uniformity of the screen.

A. Brightness Gain

The angular brightness of a projection screen is best described in terms of brightness gain, $B(\theta)$, which is the ratio of measured brightness of a screen to the brightness of an ideal Lambertian screen, as a function of angle, and with the same incident irradiance. Brightness gain rather than energy gain was chosen because of the need to describe, in general and in meaningful terms, the angular viewing properties of rear projection screens. The brightness gain is related to the angular intensity distribution $I(\theta)$ by

$$B(\theta) = \frac{2\Pi\ I(\theta)}{I_o\ \mathrm{Cos}\theta} \quad , \qquad (1)$$

where I_o is the incident irradiance. Expressed another way, the angular brightness gain is the ratio of the

energy gain of a screen to the energy gain of the Lambertian diffusor which for the latter is 2 Cosθ. The ideal Lambertian screen equally distributes the incident irradiance between the viewing and projection areas. Projection screens that do not diffuse as uniformly as the Lambertian reference will appear brighter over a limited range of viewing angles, therefore, within this region the values of brightness gain will exceed unity. Since a diffusing screen is a passive element and does not add energy to an image, any increase in gain above unity for one viewing region must result in a gain less than unity for some other region. Often it is convenient to talk about a screen in terms of its 'axial gain' which is the on axis value of the brightness gain function, i.e., at θ = o. In general, a low gain screen has uniform brightness over a wide range of bend angles while a high gain screen changes its brightness with small changes in bend angle.

The angular gain distribution should also be considered along with other facets of the projection and viewing configuration. The closer the screen is to the viewer, the greater the range of bend angles; also an increase in the dimensions of a screen has a comparable effect. The range of bend angles is also dependent upon the angular size of the screen as seen from the projector and is directly related to the focal ratio of the projection lens; the faster the lens, the greater is the range of bend angles. Therefore a screen with broad angular viewing properties may be required to maintain an image which has sufficient uniformity of brightness. It is important to note that the screen may be brighter for an observer directly in front of the screen than for one near the edge; however, it is more important to view a uniformly illuminated image than to view a brighter more non-uniform one, assuming the brightness is sufficient for all viewers to view

in comfort. It is important not to underestimate the significance of the visual response of the observer and the complexities of perceived brightness, color, and resolution.[17, 20-27]

It has been shown that the shape of the gain curves of various materials can be approximated by empirical formulas made up of common mathematical functions such as cosines, exponentials, and gaussian distributions.[3, 6, 28] The angular properties of the projection screens can then be summarized in terms of so-called shape factors which appear as constants in the empirical mathematical expressions. However, since no standard empirical curve, used for fitting scattering data, has attained general acceptance, the use of shape factors can only confuse matters.

B. Brightness Variation

The uniformity of screen brightness has been shown to be important in selecting a material with a particular

gain distribution. One measure of brightness variation, V, is obtained by describing the fractional change of brightness compared with the average brightness within a specified range of viewing angles, i.e.

$$B = \pm \frac{B_{max} - B_{min}}{B_{max} + B_{min}} \qquad (2)$$

where B_{max} and B_{min} are the maximum and minimum values of brightness gain within some specified range of bend angles. Such a measure is independent of the absolute brightness of the screen and is a property of the material under a particular set of viewing conditions. This type of description is necessary because the perceived brightness variation, which is related to the logarithmic response of the human eye, is dependent upon the absolute brightness of the screen. Therefore, by increasing the absolute brightness, a screen can be made to appear more uniform. This increase in brightness can be brought about by increasing the irradiance from the projector

or by making the screen smaller, since the irradiance on the screen is proportional to the inverse square of the magnification. Another way of decreasing the brightness variation of a screen is to use a material which has a broader brightness gain function. Unfortunately, the use of a screen with broader scattering properties results in a decrease in efficiency as more light is lost through backscattering, and in addition, the increase in backscattering increases the sensitivity of the screen to ambient light.

C. Efficiency

There are two measures of efficiency. The more general measure is the diffuse transmittance T_d, defined as the fraction of the incident irradiance which passes through the screen, i.e.

$$T_d = T_{spec} + \frac{2\pi}{J_0}\int_0^{\pi/2} I(\theta)\sin\theta\, d\theta \qquad (3)$$

where T_{spec} is the specular transmittance of the screen

and for practical purposes must be zero. A second, and more specific measure of efficiency, T_θ, is the fraction of the incident irradiance that is scattered within some specific viewing angle θ and is defined as

$$T_\theta = \frac{2\pi}{I_0} \int_0^\theta I(\theta) \sin\theta \, d\theta \quad . \qquad (4)$$

The choice of the limiting angle θ is dependent upon the specific application and the associated geometries. This measure has more meaning than the diffuse transmittance, because all of the scattered light not within some specific limiting viewing angle is lost, just as if the irradiance was absorbed or backscattered. It will be shown later that a plot of T_θ vs. axial gain is a good indicator of screen performance and is easily compared with theoretical predictions, independent of the specific physical properties of the screen.

The importance of screen efficiency should not be underestimated. It is well known that many projection

systems are literally burning up transparencies because of the need for a bright uniform picture over a wide range of bend angles. This situation generally occurs because either the screen is not properly matched to the projection and viewing requirements or the viewing requirements are unrealistic; in either case impossible constraints are imposed on the other parts of the display system, including the viewer. Certain losses outside of those due to picture size and the associated range of bend angles can be attributed to factors such as backscatter and reflection of projection light by the screen and its surfaces, and absorption by the transparency being projected. It has been shown that up to two-thirds of the available irradiance can be absorbed by a transparency.[25]

D. Resolution

Resolution is one of the most important screen parameters, as it limits the fineness of detail which

can be usefully projected. The resolution properties of a projection screen are best expressed by the modulation transfer function, which gives the contrast transfer characteristics of the screen as a function of spatial frequency. Details of the optical transfer function approach will not be discussed as they are well known and have been thoroughly treated by a number of authors.[29-34] It is worth noting that since the transfer function is the Fourier transform of the point spread function, any physical mechanism which causes spreading of a point image when projected onto a screen will also cause a reduction in the resolution of the screen, i.e., the broader the point image on the viewing side of the screen the lower the resolution.

The most important factors limiting resolution are the size of the scattering centers, their angular scattering characteristics, and the thickness of the scattering layer. Clearly, the thicker the screen, the

more spread out any point projected onto it will appear and there is little, if any, resolution at a spatial frequency equal to the reciprocal of the mean spacing between scattering particles. Another factor which reduces resolution is the irradiance trapped in the screen by total internal reflection. This irradiance tends to move across the screen, emerging at a variety of places, adding light where there should be none and reducing the overall contrast of the image. This trapping can also occur in the substrate on which the screen is made. Therefore, the broader the scattering function, the larger the fraction of the scattered irradiance trapped and hence, the lower the resolution.

E. Diffuse Reflectance

The diffuse reflectance of a projection screen is responsible for its sensitivity to ambient light. The greater the diffuse reflectance, the greater the sensitivity to ambient light, i.e. the greater the

fraction of incident irradiance that will be returned to the viewing area. It should be noted that this term describes only that component of the ambient irradiance which is diffusely returned to the viewing area from a projection screen, in contrast to the irradiance which might be specularly reflected as from a smooth surface. Screens with a low diffuse reflectance, i.e., .01 to .07, in a well lighted room with no projection irradiance, appear relatively dark while screens with diffuse reflectances greater than .1 appear white.

The sensitivity of a rear projection screen to ambient light is important and varies with the specific application.[4, 9] The more transmitting the screen, i.e., the less diffusing, the less sensitive the screen is to ambient light. This is an important factor because in many applications a display is to be viewed with a certain amount of room light present. If the screen is

highly transmitting, the ambient irradiance will pass through with very little being backscattered. However, if the screen is highly diffusing a significant fraction of the ambient irradiance will be backscattered to the observer thus degrading the contrast of the image. Generally speaking, the greater the difference between the ambient irradiance and screen brightness, the better will be the conditions for obtaining good quality on the projection screen. Such viewing problems have been treated in detail using groups of observers and varying screen conditions.[9, 19, 21] One common way of making rear projection screens less sensitive to ambient light is to add an absorbing material to the scattering layer of the screen. However, this solution is not only undesirable because the efficiency of the projection system is reduced, but because a significant fraction of the ambient irradiance is backscattered near the viewing surface of the screen and passes through very

little of the absorbing material. A more effective way of reducing this diffuse reflectance is by placing an absorbing layer next to the screen on the viewing side, thus insuring that the ambient irradiance passes through the absorbing layer twice. The absorbing material is now more effective, therefore less of it is required; hence the projection losses of the screen are minimized.

To see how diffuse reflectance effects resolution, let γ (R) and γ_o(R) be the contrasts of a sine wave target as a function of spatial frequency R on the projection screen with and without a given level of ambient irradiance, respectively. With no ambient irradiance, the contrast is given by

$$\gamma_o(R) = \frac{I_{max} - I_{min}}{I_{max} + I_{min}} \quad . \qquad (5)$$

Now adding an irradiance to both I_{max} and I_{min} equal to the diffuse contribution from the screen, i.e.,

$I_a \cdot R_d$, gives

$$\gamma(R) = \frac{I_{max} - I_{min}}{I_{max} + I_{min} + 2I_a \cdot R_d} \quad . \qquad (6)$$

Realizing that $I_{max} + I_{min}$ is just twice the average projection irradiance through the screen $\bar{I}_p$, the modulation transfer function of the screen, i.e. its response to ambient light can be written

$$\frac{\gamma\ (R)}{\gamma_o\ (R)} = \frac{1}{1 + \frac{I_a \cdot R_d}{\bar{I}_p}} \qquad (7)$$

Curves of $\gamma\ (R)/\gamma_o\ (R)$ are plotted in Fig. 2 as a function of R_d for different values of $I_a/\bar{I}_p$.

III. Theory

A. Theoretical Model

A theoretical model of rear projection screens is proposed which is based on single scattering by independent spheres as described by G. Mie.[35] This description of light scattering is used to predict the angular distribution of energy within a scattering material and from this the optical and viewing properties are calculated. For completeness, the equations summarizing Mie's theory of light scattering are given.[36] Following Chu, Clark and Churchill, the scattered irradiance for the normal and parallel components of the scattered electromagnetic field are

$$I_{\parallel}(\theta) = \left[\sum_{n=1}^{\infty} \{A_n[x\pi_n - (1 - x^2)\pi_n'] + B_n\pi_n\}\right]^2, \quad (8)$$

$$I_{\perp}(\theta) = \left[\sum_{n=1}^{\infty} \{A_n\pi_n + B_n[x\pi_n - (1 - x^2)\pi_n']\}\right]^2, \quad (9)$$

where π_n and π_n' are the first and second derivatives, with respect to x, of the legendre polynomials $P_n(x)$ of order n with $x = -\cos\theta$, and

$$A_n = \left[\frac{(-1)^{n+\frac{1}{2}}(2n+1)}{n\,(n+1)}\right]\left[\frac{S_n(\alpha)\frac{dS_n(\beta)}{d\beta} - M^*S_n(\beta)\frac{dS_n(\alpha)}{d\alpha}}{\phi_n(\alpha)\frac{dS_n(\beta)}{d\beta} - M^*S_n(\beta)\frac{d\phi_n(\alpha)}{d\alpha}}\right], \qquad (10)$$

$$B_n = \left[\frac{(-1)^{n+3/2}(2n+1)}{n\,(n+1)}\right]\left[\frac{M^*S_n(\alpha)\frac{dS_n(\beta)}{d\beta} - S_n(\beta)\frac{dS_n(\alpha)}{d\alpha}}{M^*\phi_n(\alpha)\frac{dS_n(\beta)}{d\beta} - S_n(\beta)\frac{d\phi_n(\alpha)}{d\alpha}}\right] \qquad (11)$$

where $S_n(\alpha)$ = Riccati Bessel function = $\left(\frac{\pi\alpha}{2}\right)^{\frac{1}{2}} J_{n+\frac{1}{2}}(\alpha)$, $\phi_n(\alpha)$ = Riccati Hankel function = $S_n(\alpha) + j\,(-1)^n\left(\frac{\pi\alpha}{2}\right)^{\frac{1}{2}} J_{-n-\frac{1}{2}}(\alpha)$, and $J_{n+\frac{1}{2}}(\alpha)$ and $J_{-n-\frac{1}{2}}(\alpha)$ = Bessel functions of half integral order.

The physical parameters in this description, Fig. 3, are the angle θ' between the direction of propagation of the scattered irradiance and the direction of the incident irradiance, the size parameter α given by

$$\alpha = \pi D/\lambda \qquad (12)$$

and β, given by

$$\beta = M^*\alpha = \alpha(M - ik) \quad , \qquad (13)$$

where D is the diameter of spherical particle, λ is the wavelength of incident radiation in the embedding medium, M is the real part of the complex index of refraction M* of the scattering particles relative to the embedding medium, i.e. $M = n_p/n_g$, k is the extinction coefficient of the particle material, and i is $\sqrt{-1}$. It should be noted that the dimensionless size parameter α is the ratio of the circumference of the particle to the wavelength.

The problem of obtaining solutions to scattering problems has been simplified considerably by the existence of tables listing values of the real and imaginary parts of A_n and B_n as well as tables of the Legendre polynomials including first and second derivatives 38-41. The coefficient A_n and B_n from these tables are then combined into values of $I_{\parallel}(\theta)$ and $I_{\perp}(\theta)$ according to Eqs. (8) and (9) from which the angular distribution function $I_s(\theta')$ for a single particle is obtained

$$I_s(\theta') \propto I_{\parallel}(\theta') + I_{\perp}(\theta'). \qquad (14)$$

Hartel suggested that Eqs. (8) and (9) could be simplified in form by the repeated use of recurrence relation between the derivatives and products of Legendre polynomials.[42] Recently Chu and Churchill succeeded in rearranging these these equations and in predicting the angular properties of the radiation scattered by non-absorbing spheres in terms of a series of Legendre polynomials,

$$I_s(\theta') = \frac{1}{4\pi} \sum_{n=o}^{\infty} a_n(\alpha, \beta) P_n(\cos\theta'), \qquad (15)$$

where the coefficients a_n are functions of α and β, but not of the angle.[43-46] Although it is simpler to evaluate Eq. (15) than Eqs. (8) and (9), the tables of a_n and $P_n(\cos\theta')$ are limited while tables of A_n and B_n are more complete, i.e., they have finer divisions of M and α and cover a greater range of size parameters.

Having an analytical description of the effects of particle size and relative refractive index on the scattering function, there remains the problem of calculating the observed optical properties. Only a

portion of the scattered irradiance will emerge from the screen at its first encounter with the glass-air interface; all of the remaining irradiance will be trapped by internal reflections either partial or total. The problem of describing the exact history of the trapped irradiance is extremely difficult, however, as an approximation it has been assumed that the scattered irradiance reflected by the glass-air boundary is completely randomized by additional scattering in passing through the scattering layer. It is also assumed that half of this reflected irradiance finally emerges from the front of the screen toward the viewer, and the remaining half is backscattered toward the projector.

This approximation is reasonable in the region where the scattering function is either relatively uniform, i.e. $\alpha < 4$, or very directional, i.e. $\alpha > 8$. In the first case, the trapped irradiance is randomized in a single pass through the screen,

and in the second case, the fraction of irradiance trapped is quite small, therefore the specific distribution of irradiance has little if any effect. In the region $4 < \alpha < 8$ the amount of trapped irradiance is significant, yet after a single pass through the scattering layer this irradiance is not completely randomized. However, since only a certain fraction of the trapped irradiance is scattered into the critical angle during each pass through the screen, several passes are required before all of the irradiance if effectively randomized and finally escapes.

Using this theoretical model, the angular distribution of energy inside the glass can be written:

$$I'(\theta') = I_{\parallel}(\theta')\left[1 - R_{\parallel}(\theta')\right] + I_{\perp}(\theta')\left[1 - R_{\perp}(\theta')\right] +$$

$$+ \left\{ \int_0^{\theta_c} \left[I_{\parallel}(\theta') + I_{\parallel}(\pi - \theta') \right] R_{\parallel}(\theta') + \left[I_{\perp}(\theta') + I_{\perp}(\pi - \theta') \right] R_{\perp}(\theta') \sin\theta' d\theta' + \right. \tag{16}$$

$$\left. + \int_{\theta_c}^{\pi - \theta_c} \left[I_{\parallel}(\theta') + I_{\perp}(\theta') \right] \sin\theta' d\theta' \right\} \Big/ \frac{1}{4\pi} \int_0^{\theta_c} \sin\theta' \, d\theta'$$

where $I_{\parallel}(\theta')$ and $I_{\perp}(\theta')$ are given by Eq. (8) and (9) and where $R_{\parallel}(\theta')$ and $R_{\perp}(\theta')$ are the Fresnel reflection coefficients given by

$$R_{\parallel}(\theta') = \frac{\tan^2(\theta - \theta')}{\tan^2(\theta + \theta')} \tag{17}$$

$$R_{\perp}(\theta') = \frac{\sin^2(\theta - \theta')}{\sin^2(\theta + \theta')} \tag{18}$$

The first term in Eq. (15) is the fraction of the scattered irradiance lying within the critical angle, transmitted into the viewing area or backscattered into the projection area. The last term is composed of the scattered irradiance lying within the critical angle, either at the front or back surface and totally internally reflected. The integral in the denominator is the total solid angle into which the trapped irradiance will be uniformly distributed before being refracted through the glass-air interface and out of the screen.

Based on conservation of energy considerations, the angular properties of the scattered irradiance inside and outside of the screen can be written

$$I'(\theta) \sin\theta' \, d\theta' = I(\theta) \sin\theta \, d\theta, \qquad (19)$$

where the term on the left side describes the magnitude and angular properties of the scattered irradiance contained within a small hollow cone inside the screen, and the term on the right describes this same hollow cone after refraction through the glass-air interface.

Solving for $I(\theta)$ and using Snell's law to obtain $\sin\theta$ and $d\theta'/d\theta$, Eq. (19) can be written as

$$I(\theta) = \left(\frac{n_a}{n_g}\right)^2 \frac{\cos\theta}{\cos\theta'} \, I'(\theta') \qquad (20)$$

In terms of brightness gain $B(\theta)$, Eq. (20) becomes

$$B(\theta) = \frac{2\pi}{I_o} \left(\frac{n_a}{n_g}\right)^2 \frac{I'(\theta')}{\cos\theta} \qquad (21)$$

where I_o is the incident irradiance and is found by integration of Eqs. (16) or (19). Thus having descriptions for both the angular distribution of energy and brightness, the remaining optical and viewing properties can now be calculated.

B. Theoretical Results

Values of $I_{\parallel}(\theta)$ and $I_{\perp}(\theta)$ were computed for values of α at 1, 2, 4, 6, 8, and 10, and values of M at .8, .9, 1.05, and 1.20. The extinction coefficient in all calculations was assumed zero, and to compute Fresnel coefficients, a refractive index, n_g, of 1.50 for the matrix glass was assumed. From these data were calculated the remaining optical properties.

Brightness gain curves are plotted as a function of bend angle with M = .8, for different size parameters in Fig. 4. As would be expected, the larger the particle the more directional the scattering and the greater the axial gain. The axial gain as a function of the size parameter α for different values of the relative refractive index M, is shown in Fig. 5 and is approximately given by $.862\,\alpha$ over the range of size parameters considered. The relative refractive index M does not have a strong influence on axial gain in that all values of axial gain lie within 10% of each other for $\alpha \leq 8.0$. A broader

spread of axial gain values can be expected for values of M further from unity.

As the size parameter increases, the geometrical cross-section becomes more efficient in producing scattering. This point is not obvious and furthermore is only correct for a certain range of α. To better understand this, consider Fig. 6, where the scattering coefficient K, which is the ratio of the scattering cross-section in producing scattering, is plotted as a function of the size parameter for different values of the relative refractive index. In the region $\ll 1$, the scattering coefficient can be written as

$$K = \frac{8}{3}\pi\alpha^4 \left| \frac{M^2-1}{M^2+2} \right|^2 . \qquad (22)$$

It can be seen from Eq. (22) that in this region the geometrical cross-section is not only small but is not efficient in producing scattering. This is the Rayleigh scattering region where the scattering coefficient is proportional to γ^{-4}. Because of this strong wavelength

dependence, Rayleigh scattering in a screen should be avoided. For larger particles $1 \leq \alpha \leq 10$, the geometrical cross-section becomes larger, and the scattering coefficient is near to unity. For large values of α i.e., $\alpha > 10$, the scattering coefficient oscillates and approaches an asympototic value of 2.

A range of size parameters will exist if there is a range of particle sizes and/or if polychromatic illumination is used. Both effects must be taken into consideration in estimating the expected axial gain of any given screen material. With polychromatic illumination, the range of size parameters is responsible for the color fidelity properties of the screen. This is primarily because the scattering coefficient is different for different size parameters, at least in the range $\alpha \leq 10$. The fraction of the incident irradiance, not scattered after passing through a thickness T of material with a particle density ρ is

$$I/I_0 = EXP-[K\pi D^2 \varphi T/4] \qquad (23)$$

Since the scattering cross-section is larger for the shorter wavelengths, these will be scattered more than the longer wavelengths. Color fidelity problems are easily detected by comparing the spectral energy density at two different scattering angles, for example on axis and at 45°. This phenomena is sometimes so apparent that it can be detected by a visual comparison, where the screen appears reddish when viewed on axis and bluish at some other bend angle. All volume scattering materials will display this effect in varying degrees.

The brightness variation V, based on a maximum bend angle of 45°, shows a corresponding increase with axial gain, Fig. 7. The curve intercepts the coordinate axis at an axial gain of 1.2, which corresponds to a uniformly bright screen. For values of axial gain of 1.2 or less the brightness variation remains constant while efficiency decreases with decreasing axial gain. It is important to note that the calculated data for the given range of values of relative

refractive indices and particle size parameters were used to construct the theoretical curve and that all values of V are within one percent of the curve given. The value of 45° for the limiting bend angle was chosen as representative of many commonly used viewing geometries although a theoretical curve for any other bend angle could have been computed using the data given in Fig.4.

The desirability of containing as much of the scattered irradiance within some limiting viewing angle has already been established. Fig. 8 shows the theoretical limits for the fraction of scattered irradiance contained within solid angles with half widths of 45° and 90°, i.e. T_{45} and T_{90} from Eq.(4), as a function of axial gain. The rapid increase of T_{θ} for axial gains less than 4 indicates that extra care is necessary when designing or choosing a low gain projection screen because of the rapid trade-off of usable energy with axial gain. The upper limit of the T_{θ} curves is at about 94 percent and is set by Fresnel reflections of the projection irradiance entering the screen.

An approximation to the diffuse reflectance, i.e. the sensitivity of the screen to ambient light, can also be obtained from this theoretical model. Ambient irradiance can be expected to be incident on the screen at all angles, however, because of refraction, the extreme ray passing into the screen cannot exceed the critical angle. By averaging over all possible angles, the path length of the average principal ray through the screen is not more than 20 percent greater than the screen thickness. Since the path length is not significantly longer, the scattering properties of the screen for the ambient irradiance should not differ from those values already calculated. Therefore the fraction of projection irradiance returned into the projection area is the same as the fraction of the ambient irradiance returned to the viewing area. Thus for a screen with no absorption, the diffuse reflectance is

$$R_d = 1 - T_{90} \quad , \qquad (24)$$

As with T_{90}, the major change in the diffuse reflectance occurs for values of axial gain less than 4 and varies only slowly with axial gain beyond a value of 7. The tradeoffs here are of particular importance because of the low values of diffuse reflectance required in many applications to view a display in a lighted room.

V. EXPERIMENTAL RESULTS AND CONCLUSIONS

In addition to the theoretical studies just described, an extensive experimental program was undertaken to test the validity of the theoretical work and to identify materials suited for use in rear projection screens. A class of materials known as glass-ceramics were chosen for the study owing to the great variety of crystal sizes, to the relative refractive indices between the crystals and glass, and to the number densities which could be controlled by composition and subsequent heat treatment processes. Figure 9 is an electron micrograph of one glass-ceramic material and illustrates the wide range of physical properties available by varying only the heat treatment. Crystals with refractive indices relative to air between 1.3 and 2.0 were grown in a wide range of these special glasses.

Over 100 different glass-ceramic materials and most of the commercial rear projection screen materials have

been obtained and their optical properties measured under carefully controlled conditions using polychromatic illumination. A summary of values of T_{45} plotted against axial gain is shown in Fig. 10. It can be seen that the Corning materials are in agreement with the theoretical calculations. Some Corning materials not in the main group either displayed incomplete scattering or multiple scattering. There was comparable agreement between theory and the T_{90} data plotted against axial gain; in both instances, the commercial materials were below the theoretical curves. Consider next the diffuse reflectance as a function of axial gain, Fig. 11. Materials which lie above the curve display an excessive diffuse reflectance usually resulting from multiple scattering. Those materials lying below the curve have lower diffuse reflectances than expected, and many of the commercial screen materials which constitute this group contain various amounts

of absorbing material. The presence of this absorbing material accounts for both the lower values of T_{45}, T_{90}, and R_d. Originally these materials had higher axial gains and higher values of diffuse reflectance. One possible difficulty with adding an absorbing material to a high-gain screen is that the original brightness variation remains unchanged.

Electron photomicrographs have confirmed the relationship between the particle size parameter and the brightness gain distribution given in Fig. 4, however in only a small fraction of the samples were the particle sizes measured. The advantages of comparing the different parameters as a function of axial gain, where the dependence on the diameter and the relative refractive index of the scattering particles is implicit rather than explicit, is that only optical measurements are required to compare the optical viewing properties of any material with the theoretical calculations.

One other important point is that the theoretical data in the final analysis, must be interpreted in terms of the response of the human visual system. As an example, a brightness variation of ± 50 percent over a ± 45° viewing angle may seem quite large, however in practice it is not unrealistic and a brightness variation of ± 20 percent over ± 45° is almost undetectable. A second example has already been discussed concerning diffuse reflectance and the apparent whiteness of a screen when viewed under ambient light conditions. Lastly, it is often difficult to detect differences between two screens, not side-by-side having similar angular properties and differing in efficiency by as much as 50 percent.

The author would like to express his appreciation to Dr. G. K. Megla for suggesting the problem, and to G. M. Presson for assisting with the Computer programming and the countless hours spent making the necessary measurements; also to R. F. Adrion for helpful discussions.

LL-39
12/4/67
R. B. Herrick

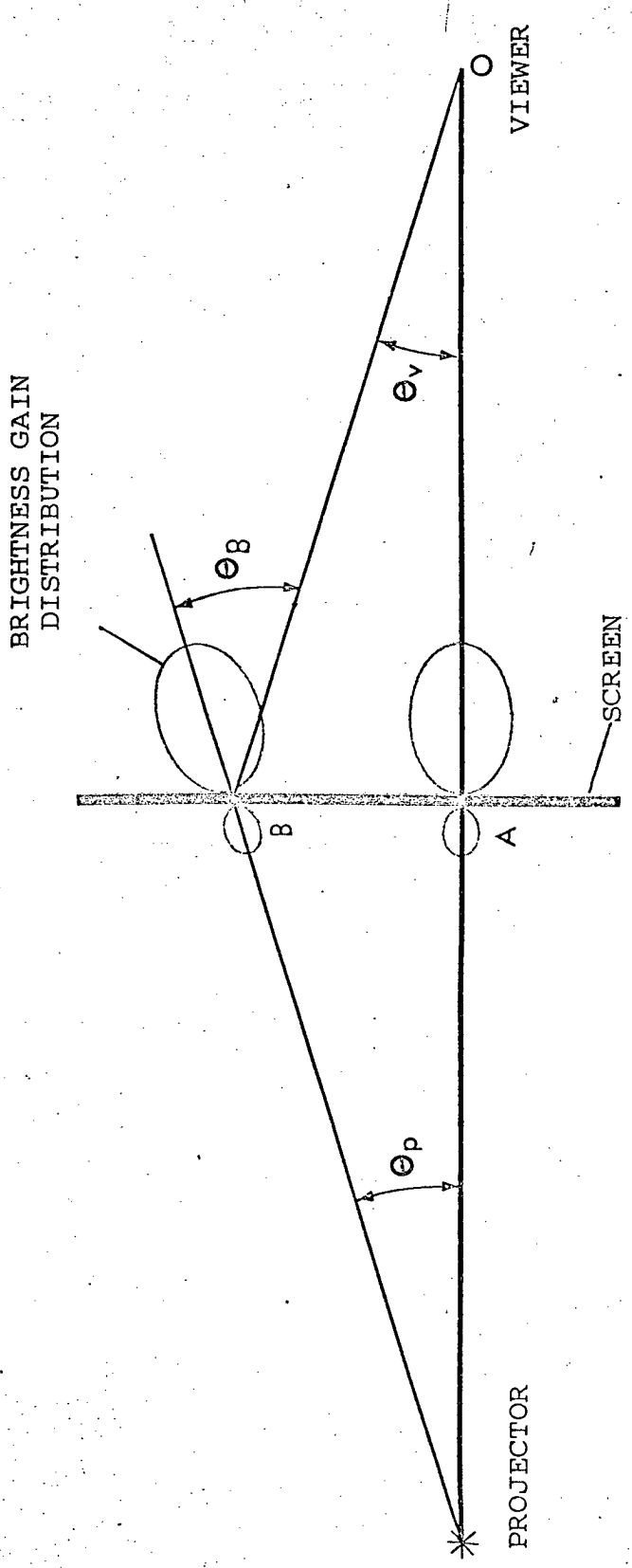

Fig. 1. Projection and viewing geometries for a a rear projection screen.

LL-39
12/4/67
R. B. Herrick

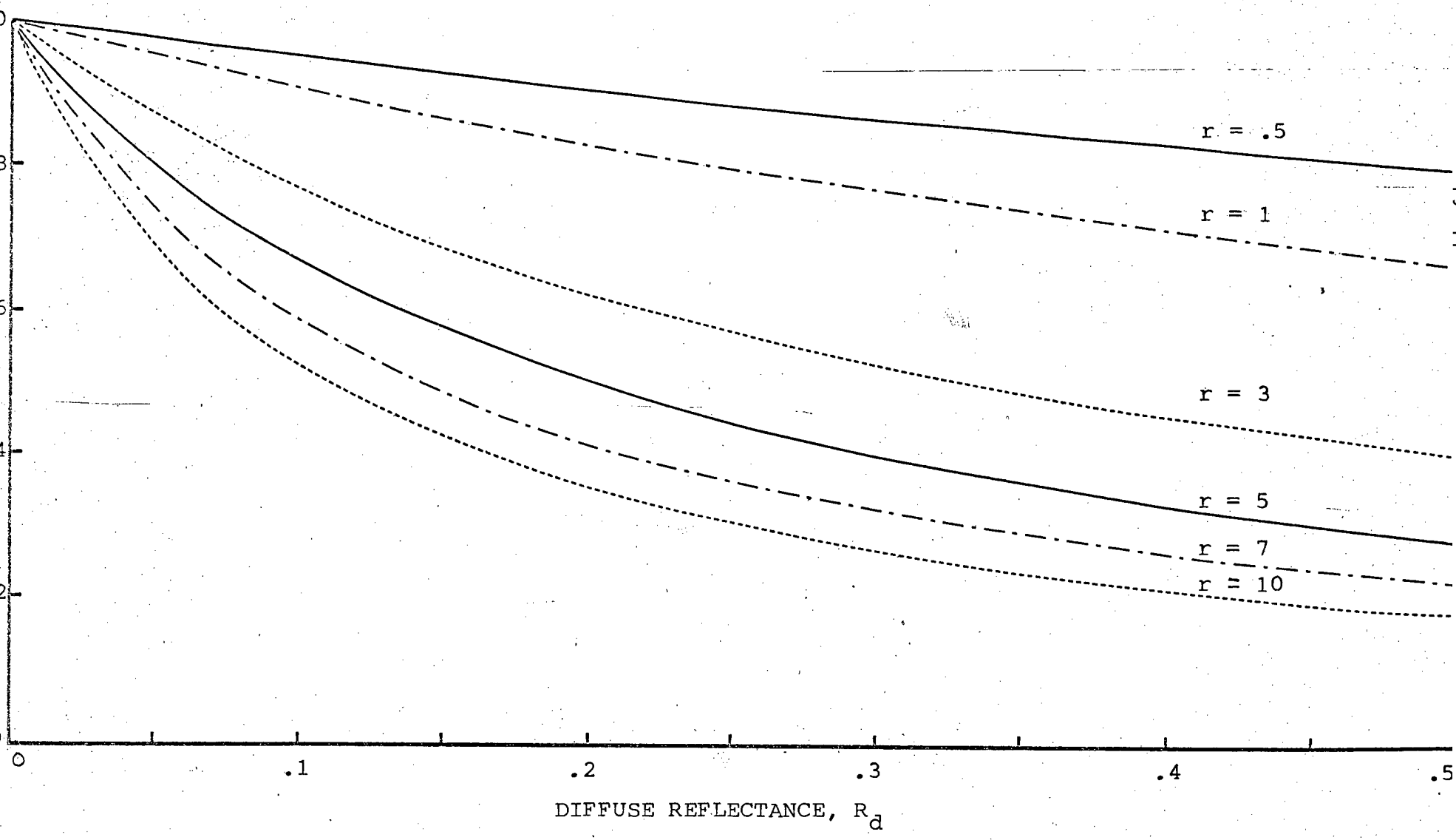

Fig. 2. Transfer function vs diffuse reflectance for different values of the ratio r, $r = I_a/\bar{I}_p$.

Declassified in Part - Sanitized Copy Approved for Release 2012/11/08 : CIA-RDP79B00873A002000010020-0

LL-39
12/4/67
R. B. Herrick

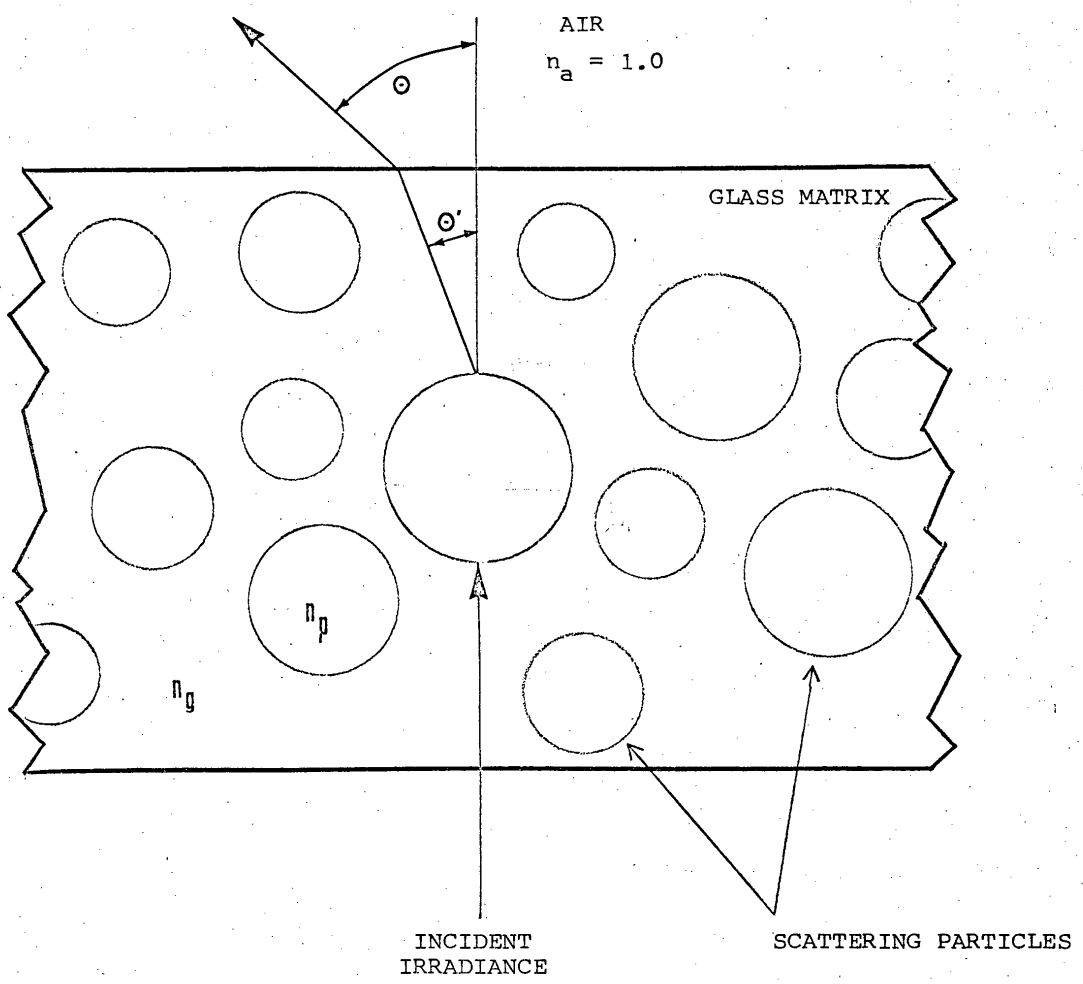

Fig. 3. Schematic view of a rear projection screen showing

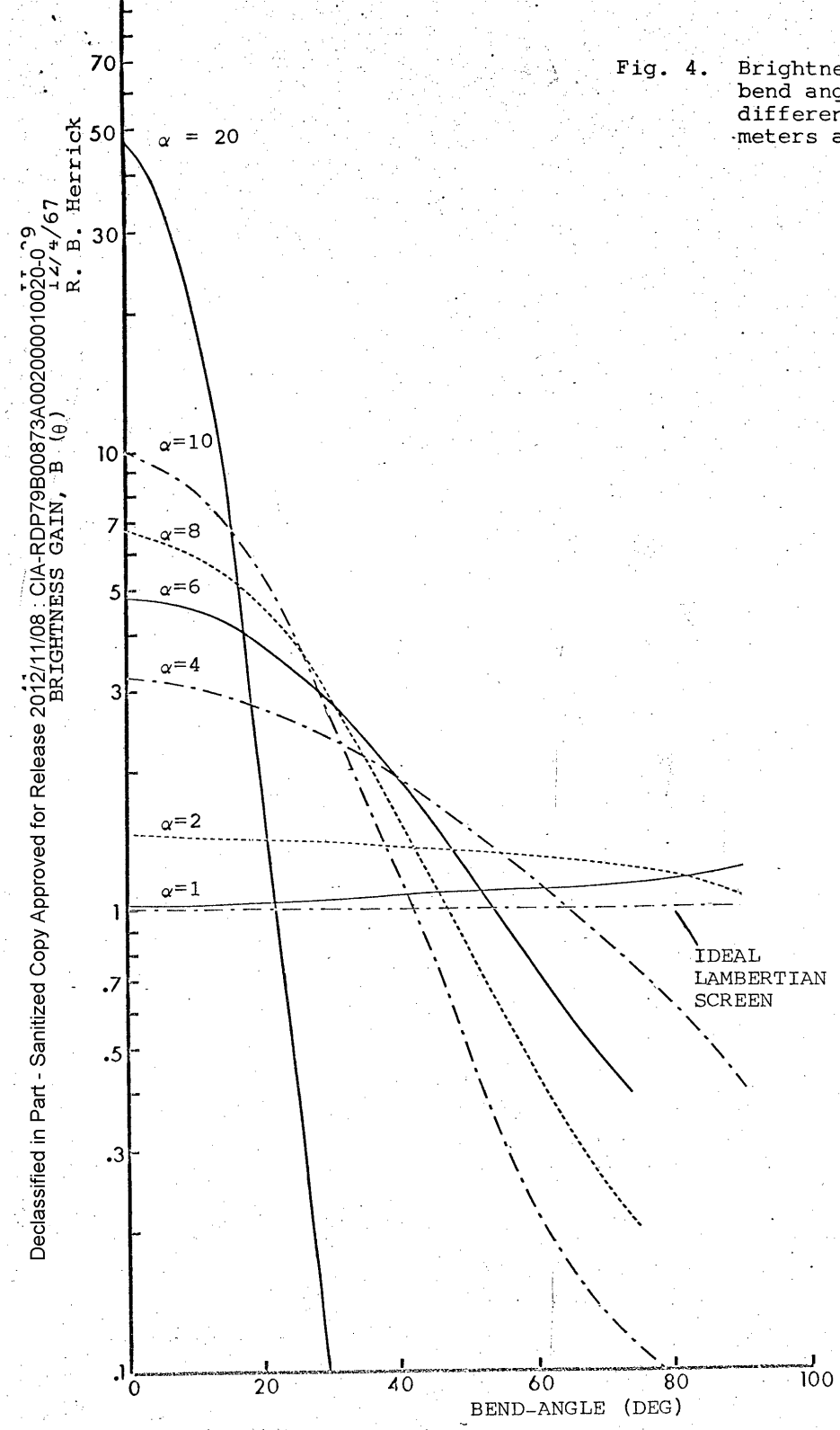

Fig. 4. Brightness gain vs bend angle for different size parameters and M = .8.

Declassified in Part - Sanitized Copy Approved for Release 2012/11/08 : CIA-RDP79B00873A002000010020-0

LL-39
12/4/67
R. B. Herrick

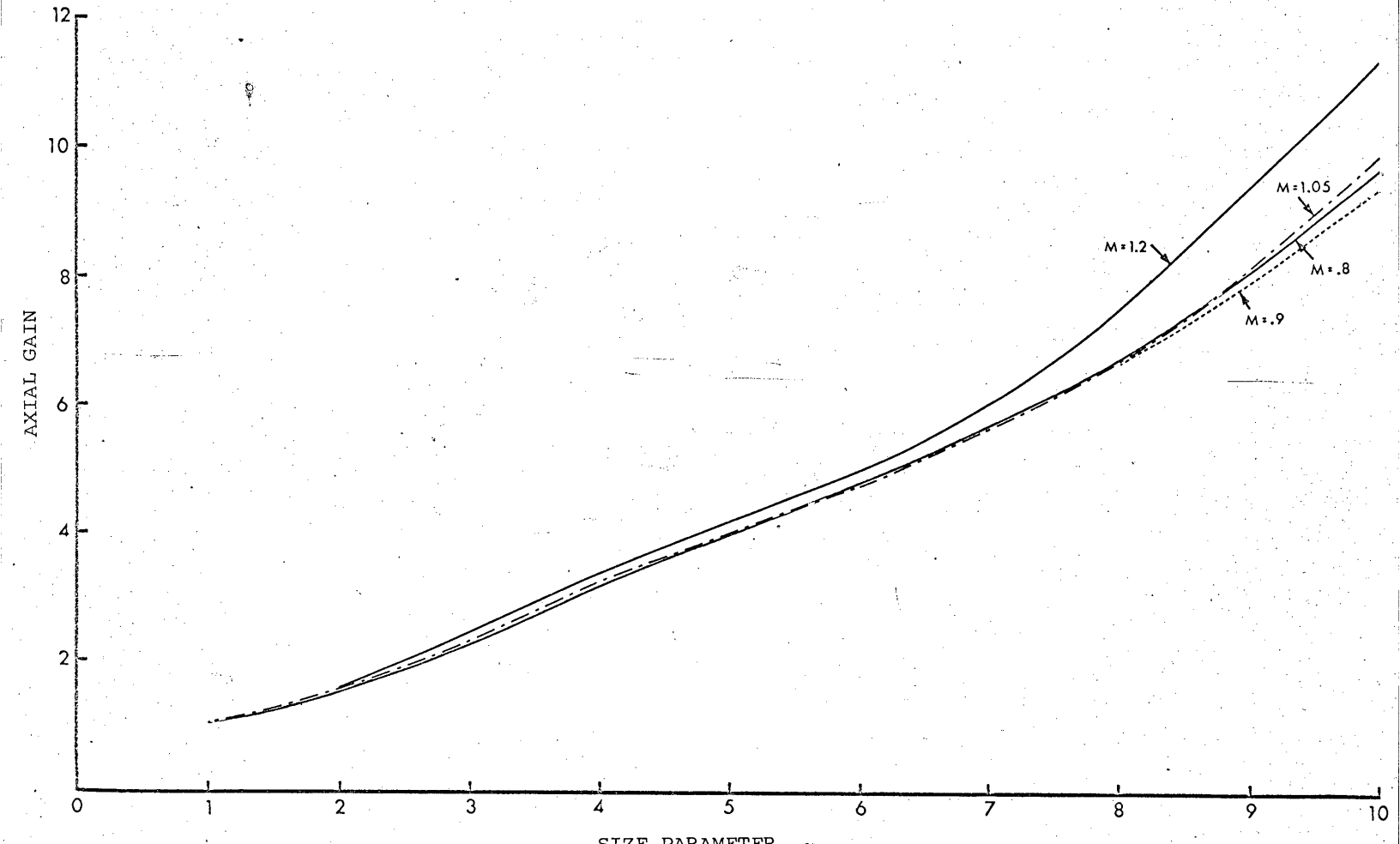

Fig. 5. Axial gain vs the size parameter α for different values of the relative refractive index, M.

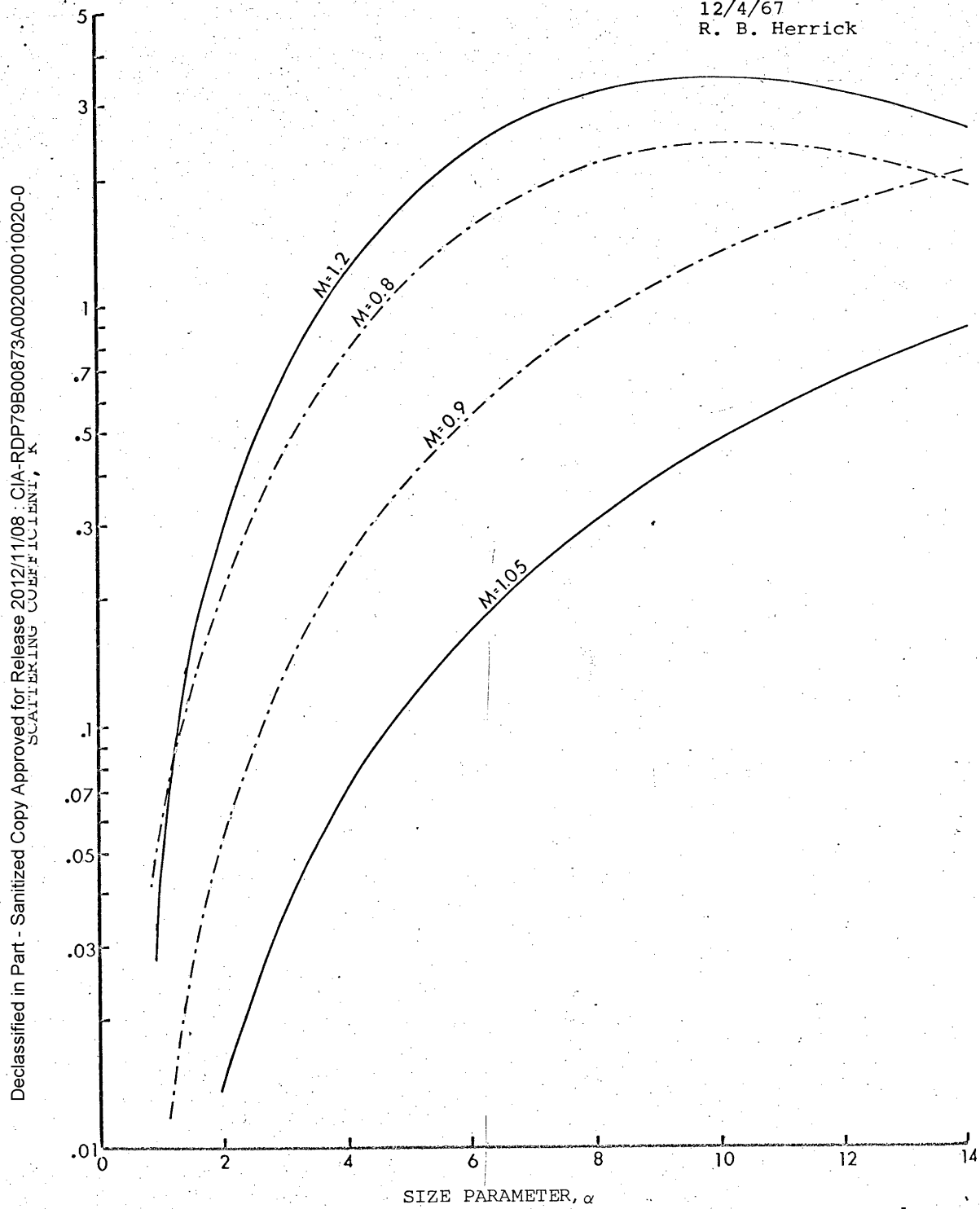

Fig. 6. Scattering coefficient vs size parameter for different values of the relative refractive index, M.

Declassified in Part - Sanitized Copy Approved for Release 2012/11/08 : CIA-RDP79B00873A002000010020-0

LL-39
12/4/67
R. B. Herrick

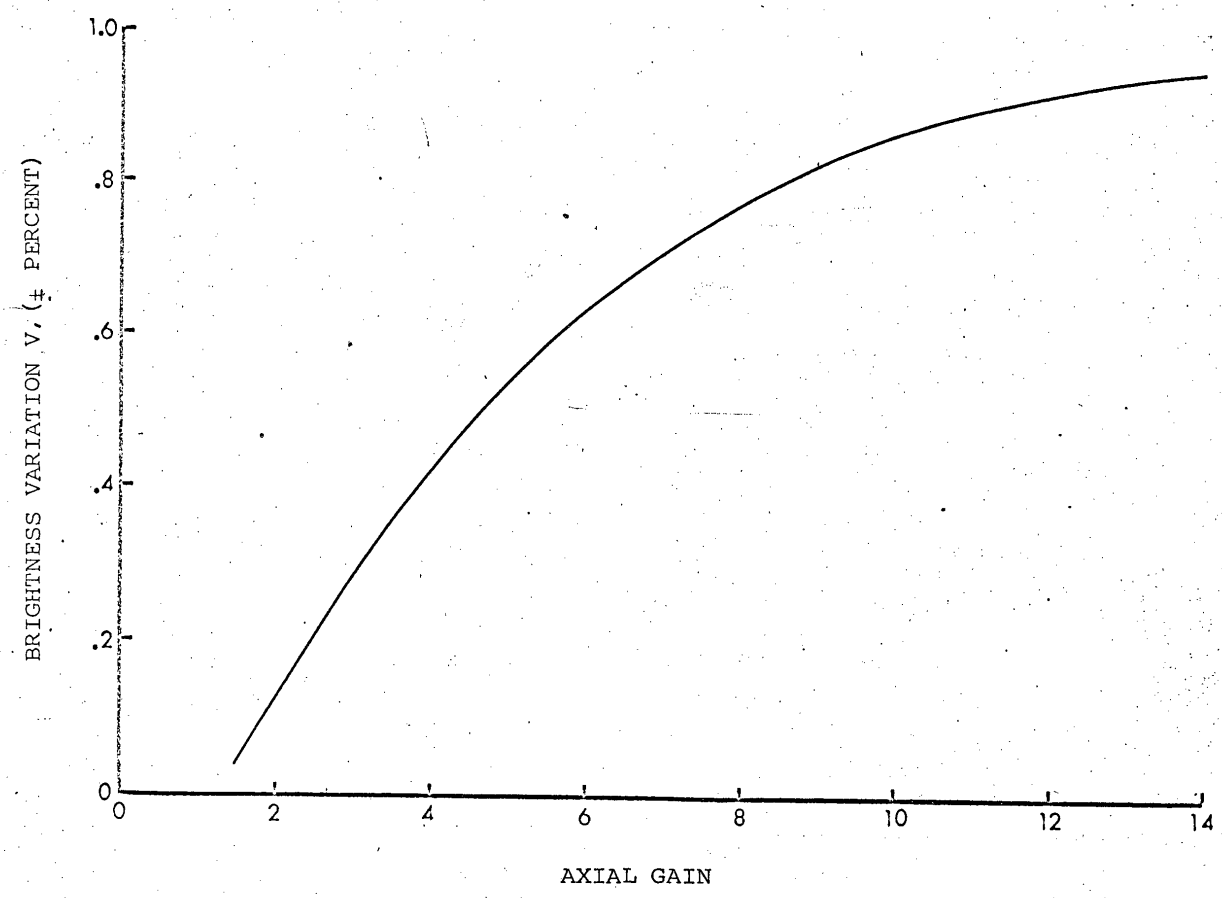

Fig. 7. Brightness variation vs axial gain.

LL-39
12/4/67
R. B. Herrick

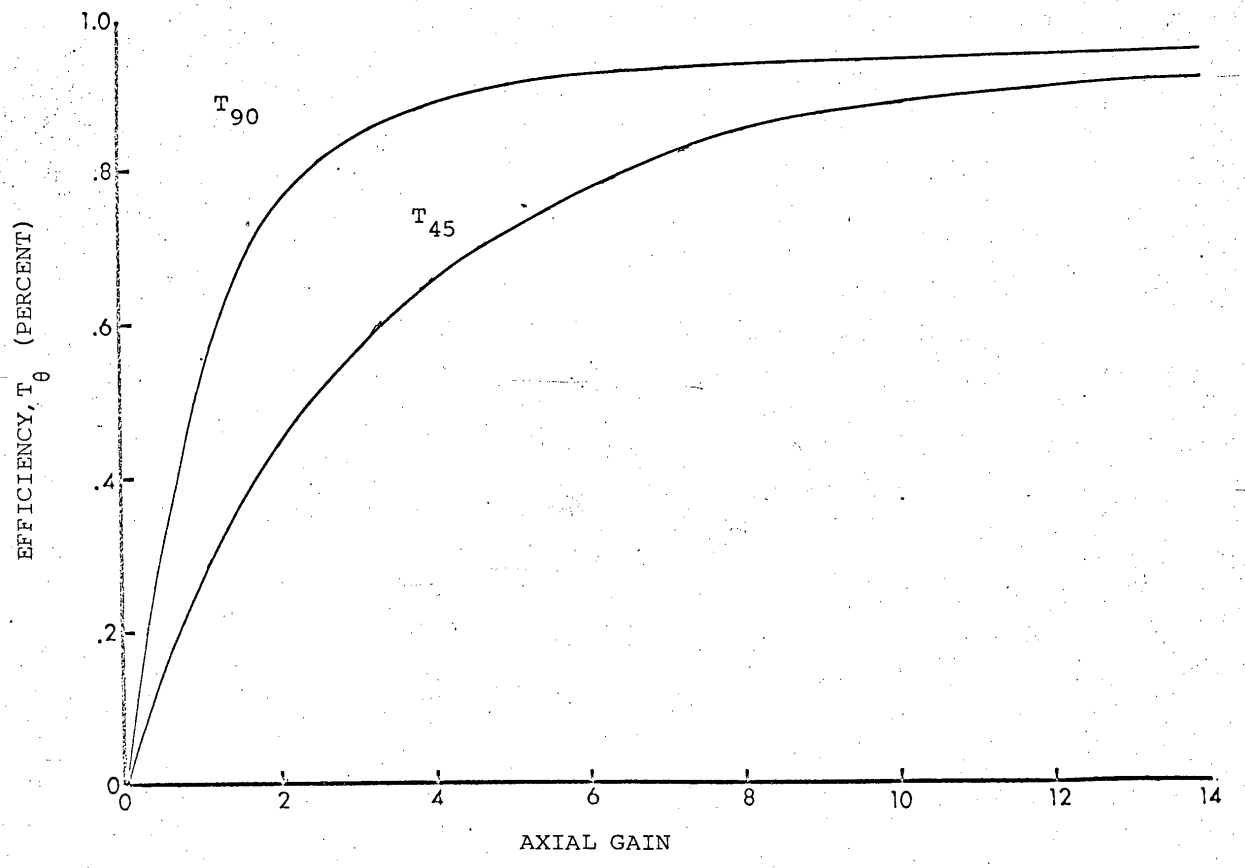

Fig. 8. Two measures of screen efficiency, T_{45} and T_{90}, vs axial gain.

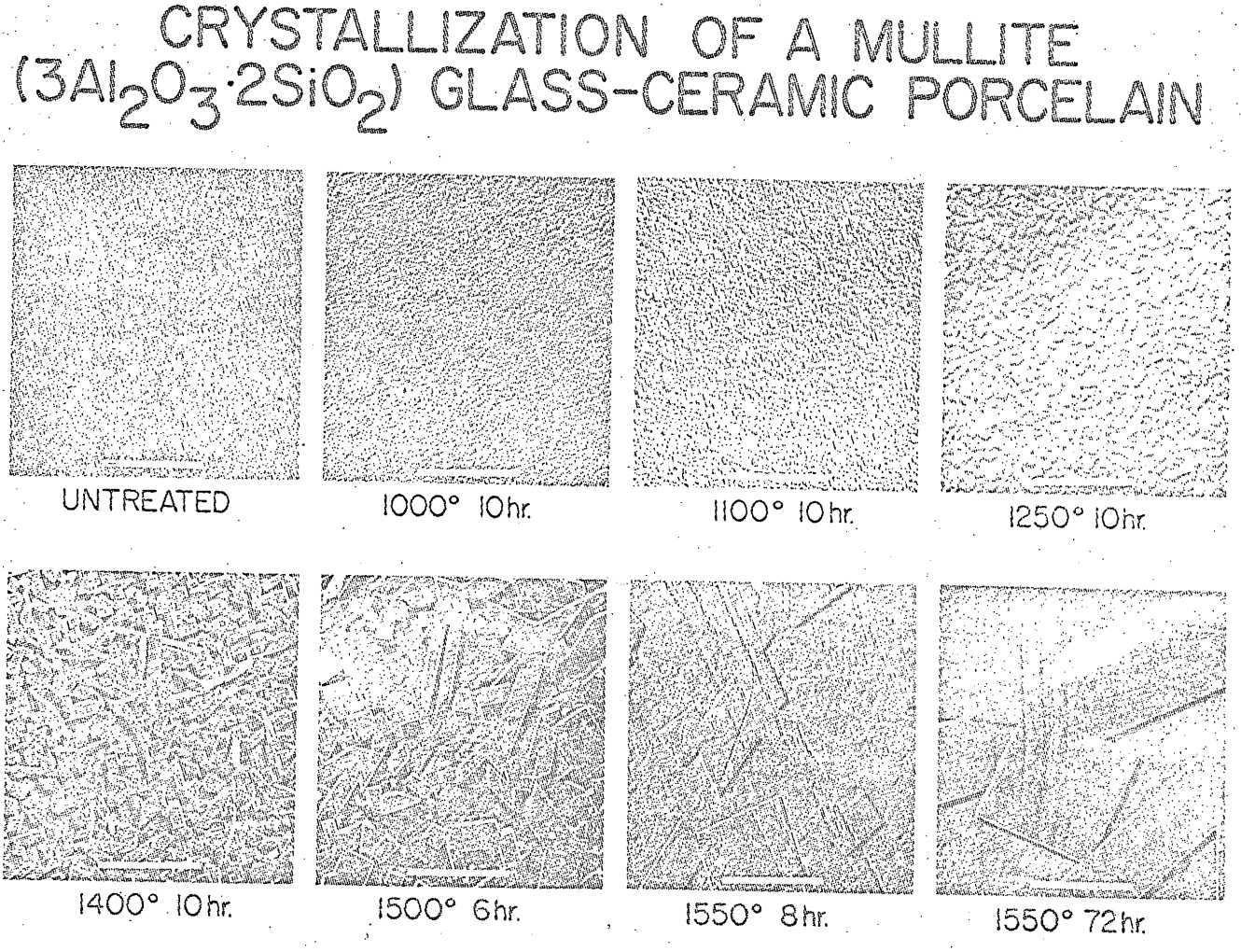

Fig. 9. Electron micrograph showing the wide range of physical properties available by only changing the heat treatment process. The white bar represents one micron.

LL-39
12/4/67
R. B. Herrick

LL-39
12/4/67
R. B. Herrick

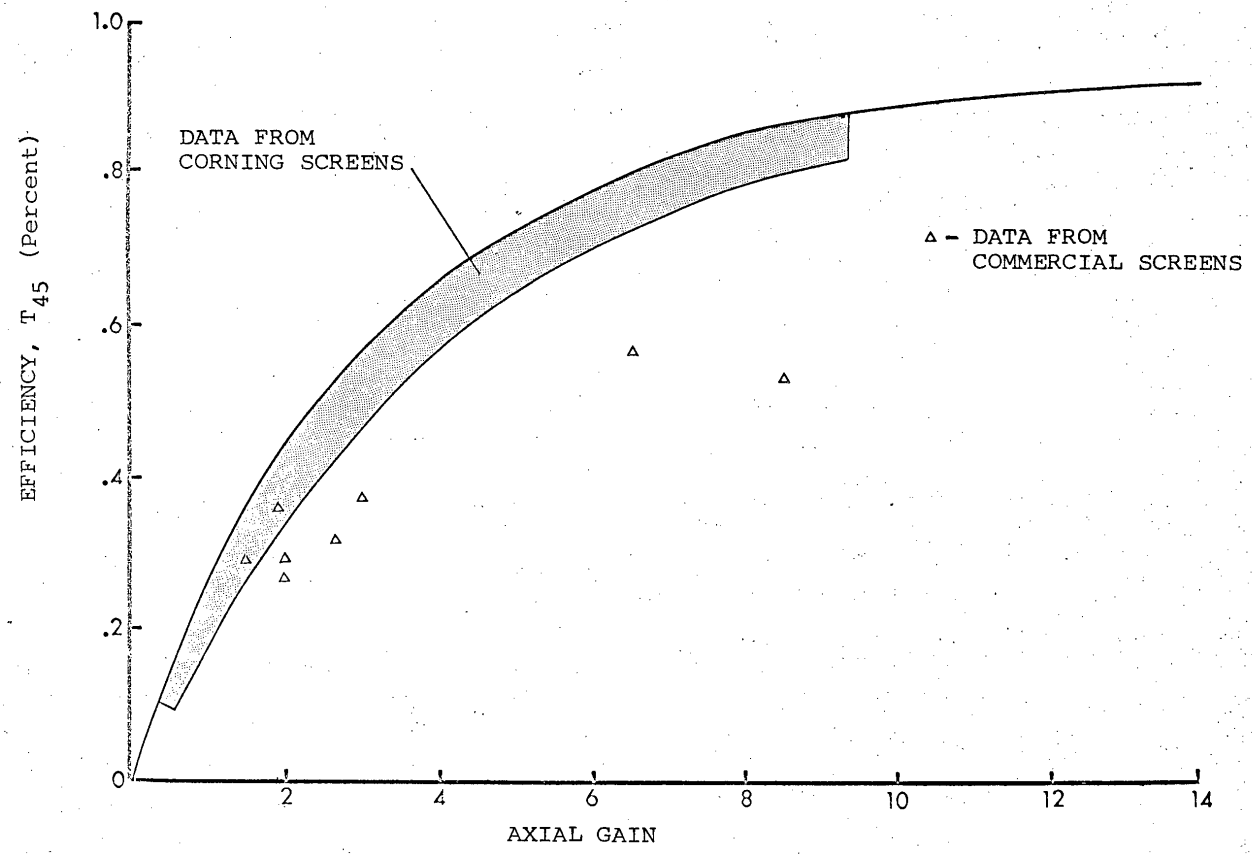

Fig. 10. Comparison of measured T_{45} values with theoretical data, from both Corning's glass-ceramic materials and from some commercial rear projection screens.

LL-39
12/4/67
R. B. Herrick

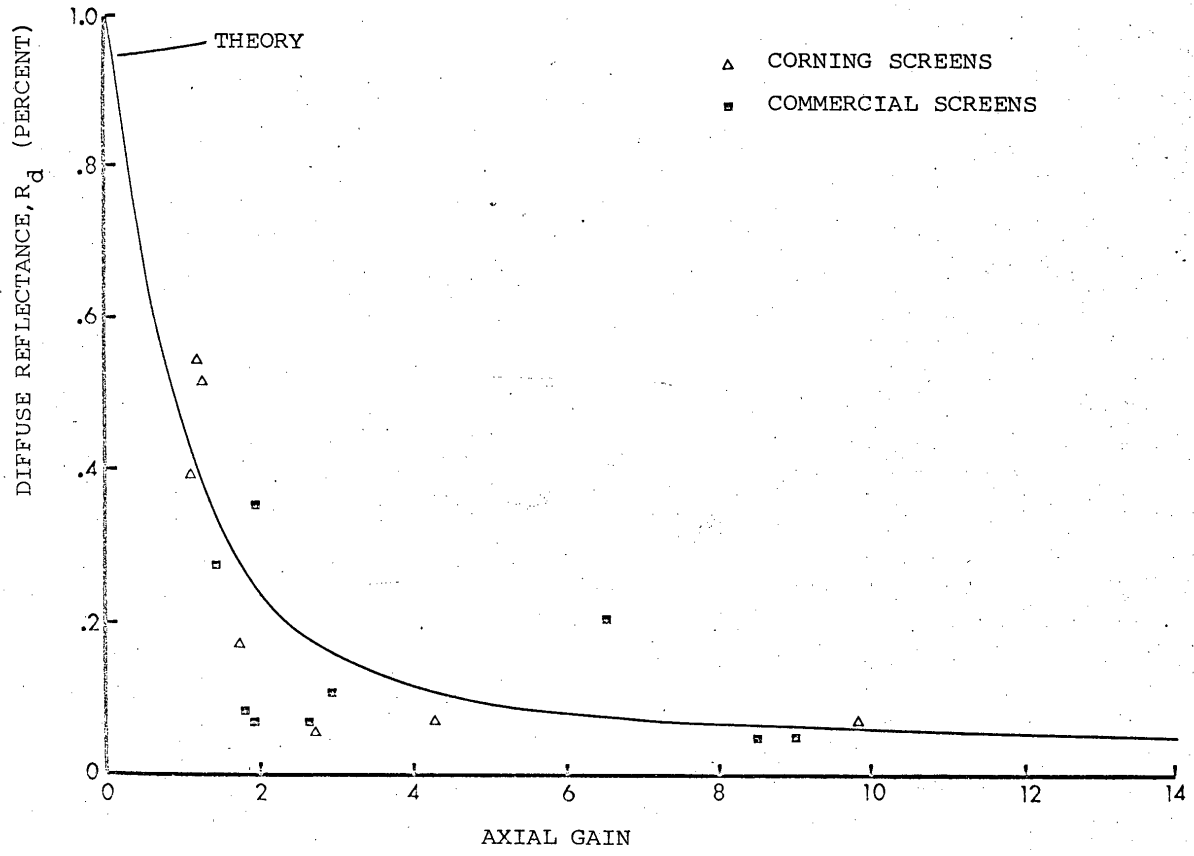

Fig. 11. Diffuse reflectance vs axial gain.

REFERENCES

1. P. Vlahos, J. SMPTE, 70, 89 (1961).

2. L. T. Sachtleben, ASTIA Report 277-746, May 7, 1962.

3. A. J. Hill, J. SMPTE, 66, 393 (1957).

4. J. F. Dreyer, J. SMPTE, 68, 521 (1959).

5. F. B. Berger, J. SMPTE, 55, 131 (1950).

6. G. Schwesinger, J. SMPTE, 63, 9 (1954).

7. G. Schwesinger, Phot. Eng., 5, 172 (1954).

8. H. McG. Ross, British Kinematography, 16, 189 (1950).

9. R. L. Estes, J. SMPTE, 61, 257 (1953).

10. E. W. D'Arcy and G. Lessman, J. SMPTE, 61, 702 (1953).

11. C. R. Daily, J. SMPTE, 65, 470 (1956).

12. Y. G. Hurd, J. SMPTE, 66, 340 (1957).

13. J. H. O. Harries, Electronics, 35, 33 (1962).

14. A. A. Cook, J. SMPTE, 44, 522 (1936).

15. F. J. Kolb, Jr., J. SMPTE, 61, 533 (1953).

16. A. J. Hill, J. SMPTE, 67, 144 (1958).

17. H. Hartridge, Photographic Journal, 115, 81 (1958).

18. H. Hartridge, Photographic Journal, 100, 81 (1960).

19. B. O'Brien and C. M. Tuttle, J. SMPTE, 44, 505 (1936).

20. E. M. Lowry, J. SMPTE, 44, 490 (1936).

21. D. Jameson and L. M. Hurvich, Science, 133, 174 (1961).

22. R. G. Hopkinson, Nature, 181, 1076 (1958).

23. O. Bryngdahl, Optica Acta, 12, 1 (1965).

24. M. R. Null, W. W. Lozier, and D. B. Joy, J. SMPTE, 50, 219 (1942).

25. R. A. Mitchell, International Projectionist, 36, 4, (1961).

26. R. Ollerenshaw, Photographic Journal, 119, 41 (1962).

27. R. Kingslake, Applied Optics and Optical Engineering Vol. II., (Academic Press, New York, 1965).

28. A. J. Hill, J. SMPTE, 61, 19 (1953).

29. E. H. Linfoot, Fourier Methods in Optical Image Evaluation, (The Focal Press, London, 1960).

30. H. H. Hopkins, Proc. Phys. Soc., 79, 889 (1962).

31. E. L. O'Neill, Introduction to Statistical Optics, (Addison-Wesley Publishing Co., Reading, 1963).

32. F. D. Smith, Applied Optics, 2, 335 (1963).

33. R. M. Scott, Phot. Sci. & Eng., 9, 237 (1963).

34. M. Born and E. Wolf, Principles of Optics, (The MacMillan Company, New York, 1964).

35. Gustav Mie, Ann. Physik, 25, 377-445 (1908).

36. H. C. Van de Hulst, Light Scattering by Small Particles. (John Wiley & Sons, New York, 1957).

37. R. O. Gumprecht and C. M. Sliepcevich, Tables of Light-Scattering Functions for Spherical Particles, University of Michigan Press, Engineering Research Institute Publications, 1951.

38. R. O. Gumprecht and C. M. Sliepcevich, Tables of Riccati Bessel Functions for Large Arguments and Orders, University of Michigan Press, Engineering Research Institute Publications, 1951.

39. R. O. Gumprecht and C. M. Sliepcevich, Tables of Functions of First and Second Partial Derivatives of Legendre Polynomials, University of Michigan Press, Engineering Research Institute Publications, 1951.

40. G. C. Clark and S. W. Churchill, Tables of Legendre Polynomials, University of Michigan Press, Engineering Research Institute Publications, 1957.

41. R. H. Boll, R. O. Gumprecht, G. C. Clark, and S. W. Churchill, Light-Scattering Functions, Relative Indices of Less than Unity, and Infinity, University of Michigan Press, Engineering Research Institute Publications, 1957.

42. W. Hartel, Das Licht, 40, 141-43, 165, 190-91, 214-15, 232-34 (1940).

43. C. M. Chu and S. W. Churchill, J. Opt. Soc. Am., 45, 958-62 (1955).

44. G. C. Clark, C. M. Chu, and S. W. Churchill, J. Opt. Soc. Am., 47, 81-84 (1957).

45. C. M. Chu, G. C. Clark, and S. W. Churchill, Tables of Angular Distribution Coefficients for Light-Scattering by Spheres, University of Michigan, Engineering Research Institute Publications: Tables; Ann Arbor, Michigan, University of Michigan Press, 1957.